7
Waveform generator circuits

7.1 Introduction

Waveform generators make up a group of instruments which are essential to the electronic circuit designer. At the simplest level, the sine wave, square wave and triangle waveform generator, covering the frequency range from a few hertz to several megahertz, is used to measure the gain and frequency response of amplifier circuits, and as a basic timing or input signal to the kind of experimental circuits that have been discussed so far in this book. Pulse generators are also of great value for circuit testing, providing both positive and negative going pulses with very fast rise and fall times, together with the facility of a separate trigger pulse from the instrument which precedes the main output pulse by some time which may be varied. A recent book by Chiang [1] covers many of these classical topics in detail and also deals with quite advanced instrumentation and signal processing techniques that rely heavily upon waveform generation.

In recent years, laboratory instruments using digital techniques for very complex waveform generation have been introduced. In these instruments, a microprocessor is used to generate the required waveform as a continuously changing digital output of eight, or more, bits, and this digital output is then converted into the required analog output by a digital to analog converter (DAC). A striking example of such an instrument is the Hewlett–Packard 8175A Dual Arbitrary Waveform Generator [2] which can generate two quite separate outputs, or, of course, related outputs, with any waveform the user needs, subject only to the limitation that these are, in fact, made up of discrete points, of ten bit accuracy, in the voltage–time plane, and that only 50 million points per second can be generated.

In connection with such digital instruments it must always be

remembered that the process of digital to analog conversion may, in itself, call for a conventional waveform generator circuit. Precision ramp generators are found in the pick-off type of DAC, and are central to ADCs as well [3]. All digital instruments require accurate clock waveform generators, which call for the generation of an accurate square waveform from a crystal oscillator, and this is by no means a trivial problem. Many digital instruments may call for highly sophisticated interpolation techniques which are realised in hardware and involve precision ramp waveforms [4].

Coming back to the more conventional kind of signal generator that is needed in the electronic circuits laboratory, another strong influence in recent times has been the development of frequency synthesis [5]. This is essentially a digital technique which makes it possible to generate waveforms of very accurate frequency and then vary this frequency rapidly from one value to another. Neighbouring values of frequency may be very close indeed, however. When these techniques of frequency synthesis are combined with waveform generator circuit techniques, very remarkable instrument performance may be achieved. For example, Danielson and Froseth [6] have described an instrument that covers the frequency range 1 μHz–21 MHz, and gives sine, square, triangle and ramp waveform outputs, all of which may be modulated, or swept in frequency.

7.2 The choice of a fundamental waveform

The simplest signal source that may be found in the electronic circuits laboratory is the function generator. This can give a sine, square, or triangle waveform output. To build such an instrument a decision must be taken on which of these three waveforms should be the fundamental one: the waveform from which all the others will be derived.

A sine wave might be chosen as the fundamental waveform if *frequency* were the output variable of prime concern. This would be because one or more crystal oscillators would be used, and these naturally produce a sine wave output when the oscillator circuit is designed for frequency precision [7].

A square wave might be chosen as the fundamental waveform when *time* was the main interest for measurement. This would follow because very fast rise and fall times would be called for from the square wave, or pulse, output from the instrument so that time measurements could be made accurately between one fast transition and another. Similarly, rise and fall times of the response of some circuit under test can only be made if the input waveform has a much faster rise or fall time.

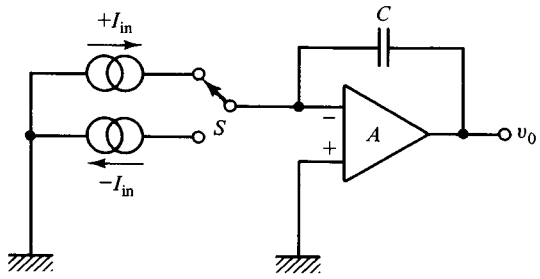

Fig. 7.1. The basic triangle waveform generator circuit.

A triangle wave might be chosen as the fundamental waveform when *rate of change* was the variable of prime concern. This would be the case when other waveforms, such as sine waves and other trigonometric waveforms, need to be generated with precision over a wide frequency range. The triangle waveform is thus the waveform usually found to be the fundamental one in a function generator. Very similar circuit techniques to triangle waveform generation are also found in ramp waveform generators and in the dual slope kind of triangle waveform generators which are so important in analog to digital conversion and in some interpolation techniques.

7.3 Triangle waveform generation

The generation of a triangle waveform usually depends upon one of the most elementary relationships of electronics:

$$i = C\mathrm{d}v/\mathrm{d}t. \tag{7.1}$$

Equation (7.1) describes the increase in the voltage, v, across a capacitor, C, when a current, i, is flowing into this capacitor. It follows that a really linear voltage ramp, with a constant $\mathrm{d}v/\mathrm{d}t$, calls for a really constant current source.

It is this provision of a really constant current source which is central to the triangle waveform generation problem. In order to produce a linear increase in v, followed by a linear decrease, it is necessary to have constant current sources of both signs and to be able to switch rapidly from one to the other.

Fig. 7.1 shows a first step towards a circuit shape for a triangle waveform generator. Two constant current generators are shown, $+I_{in}$ and $-I_{in}$, which may be switched alternately to feed the virtual earth of

https://doi.org/10.1017/CBO9781139170246.008 Published online by Cambridge University Press

an operational amplifier which is connected as an integrator by means of the feedback capacitor, C. When $+I_{in}$ flows into the virtual earth, the output voltage, v_o, will fall linearly at a rate $dv_o/dt = -I_{in}/C$. When the switch, S, is in the other position, and current I_{in} is pulled from the virtual earth, the output voltage rises linearly at a rate $dv_o/dt = +I_{in}/C$.

Fig. 7.1 does not show how the switch, S, is controlled. This must obviously be done by monitoring the output level, v_o, and changing the position of S when v_o falls to some defined level. Similarly, the switch must be returned to the position shown in Fig. 7.1 when the output subsequently rises to some level. A circuit which will provide precisely such a level monitoring and switching function has already been considered in this book: Fig. 4.6. This showed an operational amplifier with positive feedback acting as a comparator circuit and having the double valued output/input characteristic shown in Fig. 4.8. The easiest way of seeing how this circuit can be added to the basic circuit of Fig. 7.1, and so form a working triangle waveform generator, is to go at once to the first experimental circuit for this chapter.

7.4 An experimental triangle waveform generator

Fig. 7.2 shows the experimental triangle waveform generator. The constant current generators and switch, shown first in Fig. 7.1, are realised by the OP07 and the CA3019 diode array, together with their associated components. The integrator of Fig. 7.1 turns up in Fig. 7.2 as the OP27 with feedback capacitor C_1. The output monitoring and switch control part of the circuit is shown at the bottom of Fig. 7.2, and involves the wide-band operational amplifier, CA3100.

The action of the CA3100 part of the circuit shown in Fig. 7.2 is as follows. Positive feedback is applied across the CA3100 via R_7 and R_8, so that, when no current flows in R_9, the output of the CA3100 must be saturated at its maximum possible level, either positive or negative. The voltage at the junction of R_7 and R_8 is limited by two 4.7 V Zener diodes which are connected back to back. This connection gives a defined voltage level of ± 5.3 V: 4.7 V plus the 0.6 V of a forward biassed silicon diode. This means that when a voltage is applied to this part of the circuit via R_9, and R_9 is made identical to R_8, the output of the CA3100 will change sign only when the output voltage of the whole circuit, that is the output from the OP27, reaches ± 5.3 V. When v_o reaches $+5.3$ V, the voltage at the junction of R_6, R_7 and R_8 will flip from -5.3 V to $+5.3$ V. When v_o falls to -5.3 V, the voltage at this junction will flip back to -5.3 V. Naturally, other critical levels may be set for v_o by changing the relative values of R_8

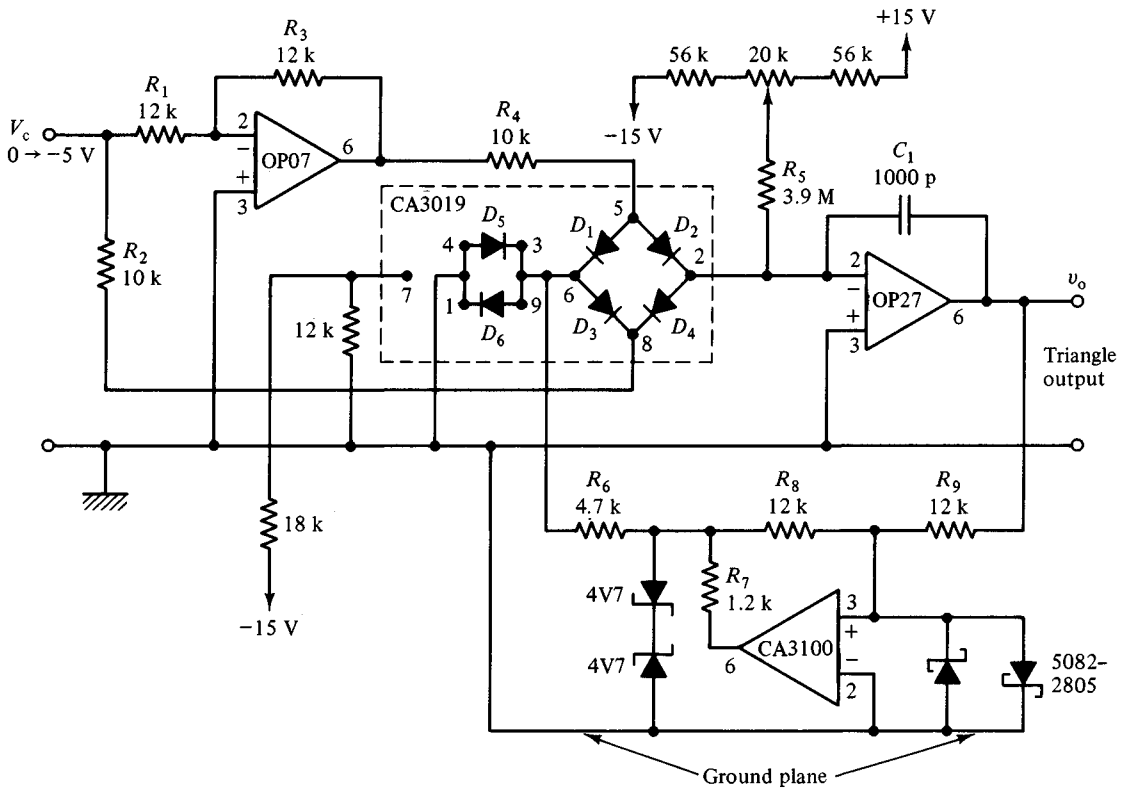

Fig. 7.2. An experimental triangle waveform generator.

and R_9. The Zener diode voltage only needs to be well below the maximum output level obtainable from a CA3100.

The CA3100 operational amplifier is thus working as a fast comparator in this circuit, a function which it performs very well indeed. It has the advantage over integrated circuits which are specially designed as fast comparators in that it naturally provides an output voltage well above or well below ground potential. It is, however, a very wide-bandwidth operational amplifier, discussed briefly in chapter 6 in connection with Fig. 6.1, and this means that this part of the circuit should be laid out very compactly with the CA3100 mounted, preferably without a holder, over a ground plane [8]. The CA3100's ± 15 V power supply pins, not shown in Fig. 7.2, must be decoupled to the ground plane with capacitors of very low inductance [9] and with the shortest possible leads. The power supply to the OP07 and OP27, also ± 15 V, must be similarly decoupled as close to the devices as possible.

Turning now to the constant current generator part of the circuit, this is implemented by noting that the constant current needs to be supplied to a virtual earth in the basic circuit first shown in Fig. 7.1. This means that a very simple solution to the problem is to provide a constant voltage, and then define the constant current by means of a resistor between this constant voltage and the virtual earth of the integrator. The value of the constant current produced in this way is then easily varied by varying the constant voltage. In this way the frequency of the triangle waveform generator may be varied or even modulated.

Fig. 7.2 shows this solution. The control voltage input is the voltage which sets the instantaneous frequency of the triangle waveform generator and is a *negative* voltage level, V_c. Ideally, this voltage would pull a current V_c/R_2 out of the virtual earth of the OP27 when the switch was in one position and supply a current V_c/R_4 to the virtual earth of the OP27 when the switch was in the position shown in the basic circuit, Fig. 7.1. The OP07 operational amplifier is being used simply as an inverter, by making $R_1 = R_3$, to provide a constant voltage equal and opposite to V_c at the input end of R_4. For a triangle waveform, $R_2 = R_4$. Things are not quite so simple as this, however, because the switch is realised, in Fig. 7.2, by means of the CA3019 diode array, and this does not make an ideal switch with negligible on-resistance and zero voltage drop. At low frequencies, when the current in R_2 and R_4 is small, the diode switch presents an on-resistance that begins to compare with R_2 and R_4, and this switch resistance is not very well defined. This is why R_5 has been connected to pin 2 of the OP27 in Fig. 7.2. The voltage at the top of R_5 is adjusted to compensate for any asymmetry in the triangle wave, which may be

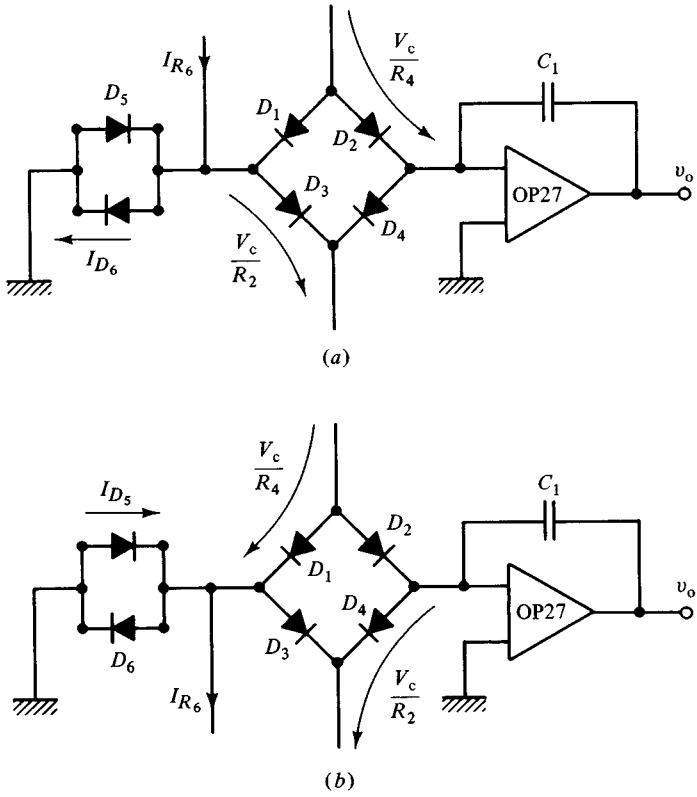

Fig. 7.3. The two positions of the diode switch which is used in the experimental triangle waveform generator.

observed at the lowest frequencies of operation, due to any difference in the on-resistances of D_2 and D_4 at very low currents. R_5 also supplies the small input bias current needed by the OP27. This may be of either sign and is only a few nanoamps.

The detailed functioning of the diode array as a switch is shown in Fig. 7.3. Fig. 7.3(*a*) shows the switch in the position first shown in Fig. 7.1, where current is supplied to the virtual earth of the integrator. In Fig. 7.2, this is the state when v_o is falling towards its lower limit of -5.3 V and the output of the CA3100 is saturated at its maximum positive level. The junction of R_6, R_7 and R_8 is at $+5.3$ V and a current, I_{R_6} will be supplied to the junction of D_1, D_3, D_5 and D_6. As shown in Fig. 7.3(*a*), I_{R_6} can only flow on, part through D_6, to ground, and part through D_3, where this part must equal V_c/R_2. For this to happen, R_6 must be chosen so that I_{R_6} exceeds V_c/R_2. The result of this, as may be seen by combining Fig. 7.3(*a*) and Fig. 7.2, is that both D_1 and D_4 have close to zero volts across them,

https://doi.org/10.1017/CBO9781139170246.008 Published online by Cambridge University Press

while D_2 is forward biassed and supplying the current V_c/R_4 to the virtual earth of the OP27. This state of affairs persists until v_o falls to -5.3 V, whereupon the output from the CA3100 changes from positive to negative, I_{R_6} reverses, and the state of the diode array goes from that shown in Fig. 7.3(*a*) to that shown in Fig. 7.3(*b*).

In Fig. 7.3(*b*) the current I_{R_6} can only flow through D_5 and D_1. In this state, it is D_3 and D_2, in Fig. 7.2, that have close to zero volts across them and D_4 now allows the current V_c/R_2 to be drawn from the virtual earth of the OP27. The output, v_o, of the OP27 thus rises towards $+5.3$ V, and, upon reaching this, the cycle repeats.

7.5 Measurements on the experimental circuit

Fig. 7.2 shows a choice of 1000 pF for C_1, which gives a maximum frequency of operation of 20 kHz for the triangle waveform generator when the input control voltage, V_c, is at about -5 V. This integrating capacitor, C_1, must, of course, be a plastic film capacitor with very low leakage.

The most revealing experiment to be made on the circuit shown in Fig. 7.2 is a measurement of its performance as a voltage controlled oscillator: the relationship between output frequency and control voltage input, V_c. This reveals the limit in the magnitude of V_c, where the current in R_6 is no longer big enough to keep the diode array switch on, and also reveals the non-linearity in the frequency–voltage characteristic due to the imperfections of the diode array as a switch.

The limit in the magnitude of V_c is best observed by looking at the voltage on pin 5, or pin 8, of the CA3019. This should be a rectangular waveform which, in the case of pin 5, is at zero during the positive slope of the triangle wave output, and at about $+0.6$ V during the negative slope of the output. As V_c is increased in magnitude, a point will be reached where V_c/R_2, referring now to Fig. 7.3(*a*), equals I_{R_6} and there is not enough current left to keep D_6 conducting. The rectangular waveform at pin 8 will then be seen to leave zero level during the negative slope of the output waveform: D_4 is no longer being turned off when it should be. The same kind of thing may be seen at pin 5 during the positive slope of the output waveform.

The non-linearity in the frequency–voltage characteristic is shown in Fig. 7.4, where the experimentally determined variation in f against the magnitude of V_c is shown, for the component values shown in Fig. 7.2. A large non-linearity can be seen for values of $|V_c|$ approaching the forward drop across the diodes, D_2 and D_4. Nevertheless, a whole decade of

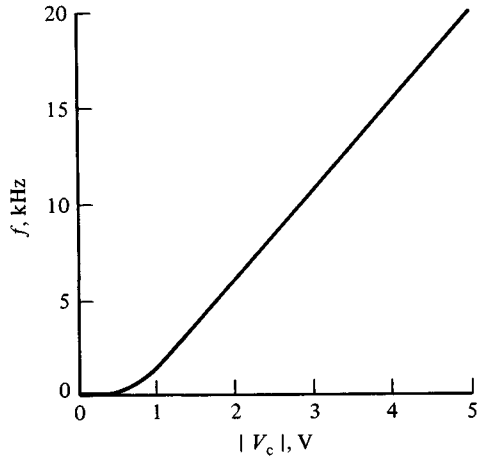

Fig. 7.4. The voltage–frequency characteristic of the experimental triangle waveform generator.

frequency, 2–20 kHz, may be covered with this circuit, and the frequency–voltage characteristic is very linear over this decade. By increasing the value of C_1 in decades, a wide range of frequency may be covered. If C_1 is made less than 1000 pF, on the other hand, slew rate limiting will eventually be observed even though the OP27 is quite a fast precision amplifier. The generation of precision triangle waveforms at megahertz frequencies is not possible using simple integrated circuits: special techniques will be called for, and these will be considered towards the end of this chapter.

7.6 A better method of output level control

A rather crude feature of the experimental circuit shown in Fig. 7.2 is the very simple way in which the amplitude of the output is set by means of the two back to back Zener diodes. This must introduce a slight temperature dependence of the amplitude of the output, which may be minimised by choosing a Zener diode that has a Zener voltage temperature dependence equal and opposite to the temperature dependence of the voltage drop across the same type of diode when in forward conduction. This choice may not, of course, be the one which would also give the required output level and, in any case, this does not help with another problem which is the fact that the current through the two Zener diodes does vary slightly as V_c is varied.

The circuit may be improved if the two Zener diodes, in Fig. 7.2, are

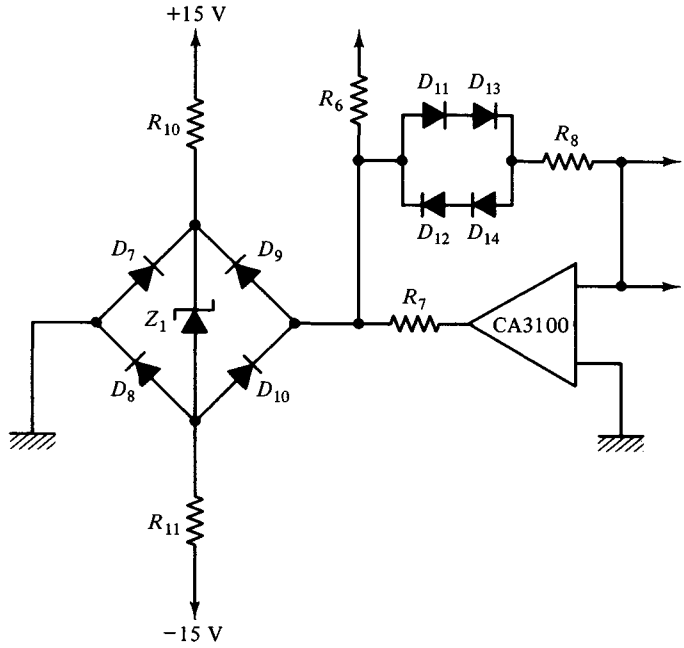

Fig. 7.5. An improvement to the experimental circuit shown in Fig. 7.2, which replaces the two Zener diodes shown there.

replaced with the rather complicated, and more expensive, connection of a precision voltage reference [10], eight diodes, and two additional resistors, R_{10} and R_{11}, as shown in Fig. 7.5. This voltage level control is far better at high frequency too, because the voltage across the voltage reference, Z_1, is always in the same direction, whereas the two Zener diodes, in Fig. 7.2, must continuously cycle between forward conduction and reverse breakdown.

Note that the forward drop across D_8 and D_9, which is, of course, temperature dependent, should be compensated by the forward drop across D_{11} and D_{13}, while D_{12} and D_{14} should compensate for the forward drop across D_7 and D_{10}. For this to happen, the forward currents of all these diodes need to be about the same, regardless of the current in R_6. This is not easy to arrange when a diode array switch is being used, because the current in R_6 will be quite large. A combination of the level control shown in Fig. 7.5 with an FET switch gets around this problem, however, and the diode currents may be made about equal by connecting a resistor from the junction of D_{13}, D_{14} and R_8 to ground [11].

7.7 Triangle to sine wave conversion

The important feature of the triangle waveform is its precisely linear rate of rise and fall. This may be exploited when some other waveform is needed as an output from an instrument which is, fundamentally, a triangle waveform generator. It is only necessary to design a non-linear circuit which has an input–output characteristic of the same shape as the required waveform, and ensure that this non-linear characteristic is independent of frequency over the required range.

A classical solution to this problem [12] is to use diodes to switch the feedback resistors across an operational amplifier, and thus change the gain as the output, or input, voltage changes. This solution is still found in quite recent instruments to solve the triangle to sine wave conversion problem [13], but it is essentially a piece-wise linear approximation and this means unavoidable discontinuities in the slope of the output waveform.

A far better solution is to use a smooth non-linearity, like the output–input characteristic of the long tailed pair circuit: the one shown in Fig. 4.5. This approach has been reviewed in an important paper by Gilbert [14], who gives a number of references to earlier work on the problem of obtaining an output–input characteristic that is an accurate match to the sine function over the range $-\pi/2$ to $+\pi/s$ in its argument.

The main problem is reproducing the zero slope that the sine function has at its maxima and minima. As Fig. 4.5 shows, the simple long tailed pair output–input characteristic approaches zero slope only asymptotically. It was, perhaps, Gilbert who first proposed the solution to this problem with a circuit of the interesting shape shown in Fig. 7.6 [15]. This effectively superimposes a number of characteristics of the kind shown in Fig. 4.5, which, alternately, have opposite sign.

As shown in Fig. 7.6, the input voltage, v_{in}, is applied directly to the long tailed pair at the centre of the circuit, Q_3 and Q_4. Referring to equations (4.1)–(4.7), it follows that Q_3 and Q_4, taken on their own, will produce a difference in output currents,

$$(i_1 - i_2)/I_L = \tanh(v_{in}/2V_T) \tag{7.2}$$

where $V_T = kT/e$, and is close to 25 mV at room temperature.

The bias current, I_B in Fig. 7.6, is arranged to produce an offset voltage,

$$V_B = I_B R \tag{7.3}$$

where R is the value of the resistors shown in Fig. 7.6. The currents in Q_1 and Q_2 are then equal when $v_{in} = +V_B$, and the currents in Q_5 and Q_6 are

https://doi.org/10.1017/CBO9781139170246.008 Published online by Cambridge University Press

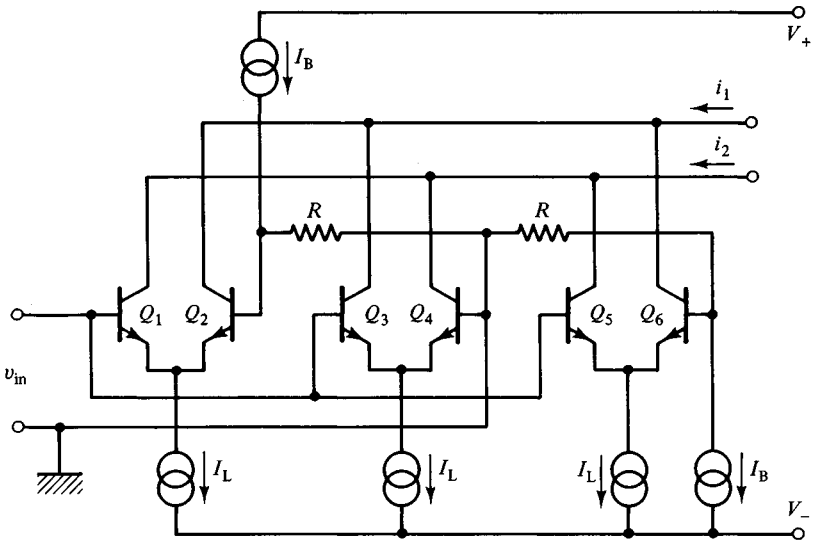

Fig. 7.6. A circuit shape which may be used to convert a triangle waveform into a sine wave.

equal when $v_{in} = -V_B$. It follows that the complete circuit shown in Fig. 7.6 has the transfer function

$$(i_1 - i_2)/I_L = \tanh(v_{in}/2V_T) - \tanh[(v_{in} - V_B)/2V_T] - \tanh[(v_{in} + V_B)/2V_T]. \tag{7.4}$$

A judicious choice of V_B can make the function given by equation (7.4) agree with the sine function to within a few per cent over the range of $v_{in}/2V_T$ which would then be used to correspond to $\pm\pi/2$. This is shown in Fig. 7.7, where equation (7.4) has been plotted for the particular case of $V_B = 75$ mV, assuming that $V_T = 25$ mV. The function shows a maximum, $+0.2923$, occurring at $v_{in}/2V_T = 0.75$, and a minimum, -0.2923, occurring at $v_{in}/2V_T = -0.75$. The function also shows an asymptotic approach to ± 1 as $v_{in}/2V_T$ tends to $\mp\infty$.

By driving the circuit shown in Fig. 7.6 with a triangle waveform of amplitude $1.5\,V_T$, this amplitude being kept strictly constant as the frequency is varied, an output $(i_1 - i_2)$ will be obtained that is a very close match to a sine wave with an amplitude of $0.2923 I_L$.

Gilbert's later developments of circuits along these lines [14], which he had termed 'translinear circuits' in an earlier work [16], led to remarkably powerful monolithic circuits which could synthesise all the standard trigonometric functions, and their inverse functions, over a much wider range of argument than the limit of $\pm\pi/2$ which has been put forward

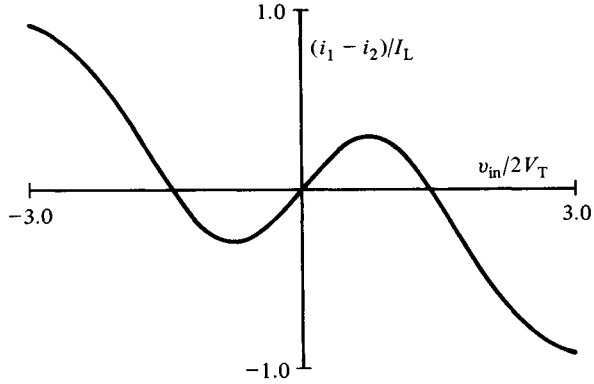

Fig. 7.7. The output–input characteristic of the circuit shown in Fig. 7.6 when $I_B R$ is made equal to 75 mV.

here [17]. These provide a solution to the triangle to sine wave conversion problem and are also the solution to many other complex waveform generation problems, even up to frequencies around 10 MHz.

7.8 Problems in fast waveform generation

So far in this chapter, only fairly low frequency waveform generators have been discussed. Even so, the experimental triangle waveform generator of Fig. 7.2 was limited in its performance by the slew rate of the operational amplifier which was used as an integrator. It is clear that the generation of triangle and ramp waveforms with frequencies well up in the 10 MHz region, or above, will call for special techniques.

Fast ramp waveforms are needed for the timebase in simple analog oscilloscopes. A 100 MHz analog oscilloscope, for example, will certainly need a timebase waveform fast enough to sweep one screen diameter in 100 ns. The actual waveform generating circuit would operate at quite low level, perhaps giving a 5 V sweep in 100 ns, and then the problem of generating the waveform which is needed to drive the CRT is shifted onto the design of the deflection amplifier, a topic which was considered in section 6.11. Nevertheless, the 5 V in 100 ns, mentioned above, is a rate of change of 50 V/μs, and this calls for special techniques.

Fast pulse waveform generation has already been considered in this book in chapter 2. There, the techniques used to generate the very short pulses needed for high speed sampling gates were discussed, and, as with most high speed switching circuits, attention was focused on the device being used: the step recovery diode. Some fast pulse and square wave generation problems are more circuit conscious, however, and an example

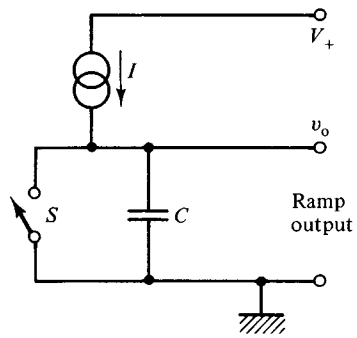

Fig. 7.8. A beginning to the solution of the fast ramp generation problem.

is the classical sine wave to fast square wave conversion problem. This was mentioned above in section 7.1, and will be the final topic of this chapter. Before that, the fast ramp or timebase waveform problem will be considered.

7.9 Fast ramp generation

The simple circuit shape shown at the beginning of this chapter, Fig. 7.1, fails when applied for very fast ramp waveform generation for two reasons.

The first reason is the limitation on the slew rate at the output of the operational amplifier. This must always be much greater than the maximum rate of change of voltage which is called for at the output, otherwise the amplifier is no longer working as a linear device.

The second limitation on the simple circuit shape shown in Fig. 7.1 is the finite propagation delay across the operational amplifier. If the switch, S, is to change position very rapidly, to produce the transition in the waveform from the positive going ramp to the negative going ramp by reversing the current flow into the virtual earth, the same rapid reversal should take place in the current flowing in the feedback capacitor, C. However, this reversal will not take place instantaneously because of the delay through the amplifier, A. This will mean that the input circuit of the operational amplifier will become saturated and a finite time will be needed for its recovery.

It follows that fast ramp waveform generation is usually tackled with a quite different circuit shape to the one shown in Fig. 7.1.

A first step towards a new circuit shape is shown in Fig. 7.8. A capacitor, C, is shown, charging from a constant current source, I, and thus producing a linear sweep, $dv_o/dt = I/C$. The sweep is initiated by

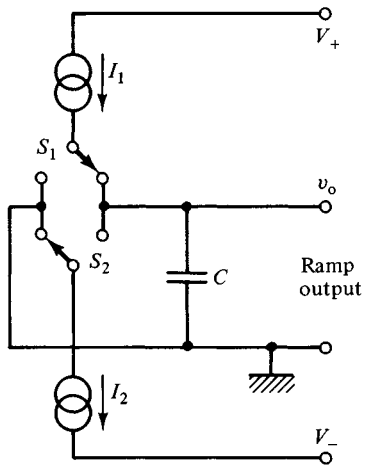

Fig. 7.9. *Fast dual-slope ramp generation.*

opening the switch, S, very rapidly, so that the current, I, is simply diverted, from flowing through S to ground, into the capacitor. The output voltage, v_o, rises linearly to some pre-determined level, where a level detecting circuit would send a control signal back to the switch, S, and make it close again. This would generate the fast resetting of the ramp output voltage: the flyback of a timebase waveform, for example. If an accurate dual-slope ramp waveform were needed, as it is in many ADC applications [3] and in the digitising oscilloscope fine interpolator, mentioned at the beginning of this chapter [4], two change-over switches would have to be used, as shown in Fig. 7.9, with two separate constant current sources, I_1 and I_2.

An important feature of both circuits, shown in Figs. 7.8 and 7.9, is that the constant current generators will always be working into a well-defined load, provided the switches are make before break switches. This is in contrast to the simple integrator idea of Fig. 7.1, where the finite propagation delay in the operational amplifier meant that the constant current generators would find themselves loaded by a saturated input circuit, instead of a true virtual earth, every time the switch, S, changed position. In fact, this problem may be seen experimentally with the circuit, Fig. 7.2, which was used earlier in this chapter. A sufficiently sensitive wide-band oscilloscope will show that the virtual earth of the OP27, used there as an integrator, is no true virtual earth at all for the fraction of a microsecond during which the triangle output waveform is changing the sign of its slope. On the rather slow time scale of this experimental circuit, however, this is no problem.

7.10 A practical circuit

Fig. 7.10 shows the practical realisation of the kind of circuit shown here first as Fig. 7.8. The constant current generator, I in Fig. 7.8, is realised in Fig. 7.10 by means of Q_1, which is in grounded base configuration with its base returned to a well-defined voltage level a few volts below V_+. This voltage level is defined by the Zener diode, D_1, while the normal silicon diode, D_2, is included to make some compensation for the temperature dependent V_{BE} of Q_1. In this way the current in Q_1 is defined at V_{D_1}/R_1, where V_{D_1} is the Zener voltage of D_1.

Q_2, in Fig. 7.10, plays the part of the make before break switch, S, in Fig. 7.8. The trigger input simply turns Q_2 either off, to initiate the ramp, or on, to terminate the ramp and discharge C_1 ready for the next sweep of the timebase. This trigger input, in a practical situation, would come from the control circuits of the oscilloscope. The negative going transition of the trigger input, which turns Q_2 off, would come from the timebase trigger circuit, while the positive going edge, which turns Q_2 on again, would be generated by some level comparator circuit in the timebase output amplifier, which would detect the fact that the CRT display had swept out a full screen diameter.

For an analog oscilloscope, the fairly simple kind of constant current source shown in Fig. 7.10 will be good enough. The timebase range will be set by switching values of R_1 and C_1; Q_2 needs to be a transistor that will switch rapidly, to minimise the delay in starting the sweep once the trigger edge has been generated. Q_2 must also have a very low leakage current when it is turned off. Similarly, the wide-band amplifier which follows this circuit should have a very high input impedance, so that negligible current is drawn from the capacitor, C_1, as the voltage across it builds up. If this were to happen the linearity of the sweep would be degraded.

The temperature dependence of the constant current source shown in Fig. 7.10 is acceptable for simple analog oscilloscope applications because a fine adjustment is always provided so that the timebase speed can be set, against the oscilloscope graticle, using an accurate internal clock waveform. The sources of temperature dependence, in the circuit shown in Fig. 7.10, are the variation of V_{BE} for Q_1, which can never be perfectly matched by the simple diode, D_2, and the variation of h_{FE} in Q_1, which will change the base current flowing from Q_1, this being subtracted from the defined current, V_{D_1}/R_1, to leave the current which actually defines the sweep speed. There is also the temperature dependence of V_{D_1} itself.

https://doi.org/10.1017/CBO9781139170246.008 Published online by Cambridge University Press

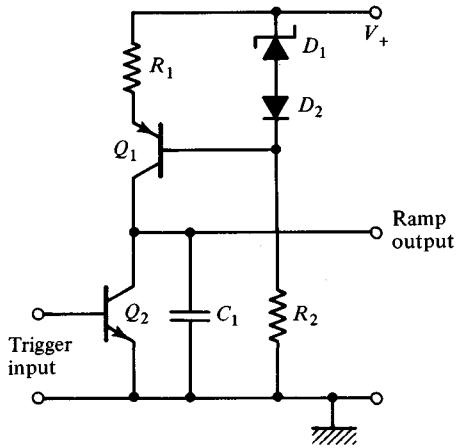

Fig. 7.10. The kind of circuit shape found in an analog oscilloscope for the timebase generator.

7.11 Precision ramp generation

When a very precise timebase waveform is called for, a much better kind of current source circuit must be developed, compared to the simple single transistor circuit shown in Fig. 7.10.

Fig. 7.11 shows the kind of circuit shape that is needed. The current source is now provided by means of a precision voltage reference, Z_1 (the same device dealt with in section 7.6 [10]), and an instrumentation operational amplifier, A_1, with a very low input offset voltage and input bias current. In this new circuit the reference voltage, V_{Z_1}, is accurately reproduced across the resistor R_1. Furthermore, the use of an MOST for Q_1, in place of the bipolar device previously used in Fig. 7.10, means that there is no temperature dependent current subtracted from the defined current, V_{Z_1}/R_1.

The use of a p-channel enhancement MOST for Q_1, in the circuit shown in Fig. 7.11, has the great advantage of putting the output voltage level of A_1 several volts below the positive rail, V_+, so that A_1 can be powered from this same positive supply.

The MOST should also have a more well-defined output capacitance, compared to the bipolar transistor of the previous circuit, and this brings up two more points which should be considered when precision ramp generators are being designed.

The first point concerns factors which may make the value of C_1 change as the voltage across it builds up. The dielectric used in C_1 must be free from any non-linearities of this kind. Ceramic dielectric capacitors are, of

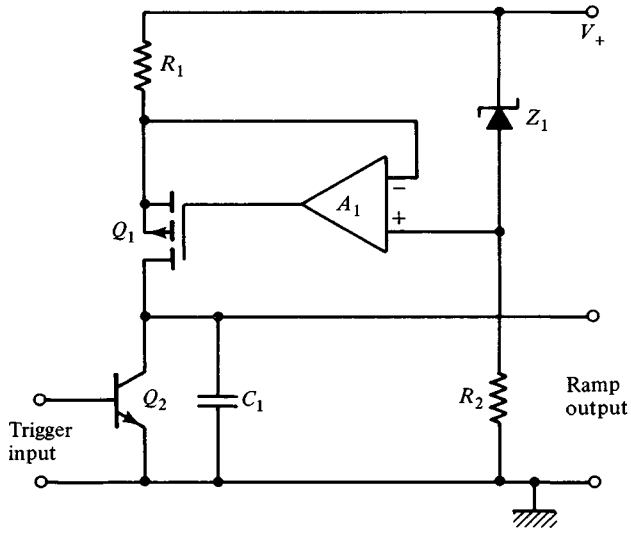

Fig. 7.11. Schematic of a timebase waveform generator circuit using a precision current source.

course, quite unusable in this respect, but it is interesting to note that many very complex non-linear and time dependent effects remain to complicate the designer's work, even when the highest quality capacitors are used [18].

The second point concerns the output capacitances of Q_1 and Q_2. These will both be in parallel with the capacitor C_1 but, because Q_1 and Q_2 will both be high frequency devices, the additional capacitance should be only a few picofarads. Nevertheless, this will impose a lower limit on C_1 because the small voltage dependent part of the output capacitances of Q_1 and Q_2 must be kept negligible in comparison to C_1. This means a lower limit of about 50 pF for C_1, and that really high speed ramp generation must call for quite high currents.

Finally, the output capacitance of Q_1 may introduce problems at very high speed because a small high frequency current can be supplied to the output of A_1 through this capacitance, and the output impedance of A_1 may well be quite high at high frequency. This problem may be overcome by using a second p-channel MOST in cascode connection with Q_1. The gate of this second device will be taken to a well-decoupled bias point, and thus will isolate A_1 completely from the fast waveform across C_1.

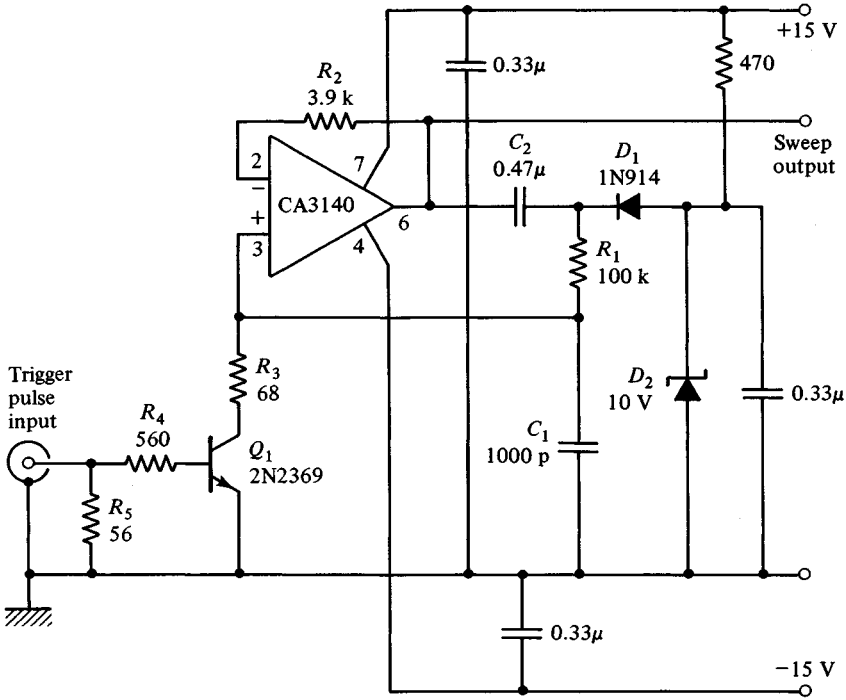

Fig. 7.12. An experimental ramp generator circuit which illustrates bootstrapping.

7.12 The bootstrap technique

The problem of providing a constant current source for precision ramp waveform generation can be solved by using a quite different technique to those described in the previous sections. This is the bootstrap technique, and is, in fact, a very old idea in electronic waveform generation [19].

As with the previous circuits, Figs. 7.10 and 7.11, constant current in a bootstrap circuit is produced by keeping the voltage across a resistor constant. The bootstrap circuit, however, exploits the fact that the ramp output waveform must be taken to the outside world through an amplifier that presents a very high input impedance to the timing capacitor, C_1 in the previous circuits, and also has a very low output impedance. This same low output impedance can then be used, after a level shift, to drive the current into the timing capacitor via the current defining resistor. The bootstrap technique is thus an example of positive feedback.

The technique should be made clear from Fig. 7.12, which shows the second experimental circuit for this chapter. In Fig. 7.12, the ramp waveform is being generated across the timing capacitor, C_1, which, as

https://doi.org/10.1017/CBO9781139170246.008 Published online by Cambridge University Press

previously, has a fast switching transistor, Q_1, connected across it. C_1 is charged by the current in R_1, and, initially, this current is defined by the Zener diode, D_2, which sets the voltage across R_1 to be 10 V, less the forward drop across D_1 and the $V_{CE(SAT)}$ of Q_1. The resistor R_3 may be ignored at this stage.

When Q_1 turns off, C_1 begins to charge. Through C_2, which is made much larger than C_1, the voltage follower (the CA3140) pulls up the top of R_1 (by its bootstraps!), turning off the diode D_1. The voltages at the top and the bottom of R_1 both rise, both at exactly the same rate if the voltage follower gain is unity, and the ramp will be linear because the current in R_1 is being kept constant by means of this bootstrap action.

7.13 Measurements on the bootstrap circuit

The values shown in Fig. 7.12 give a ramp which rises at a rate just below 0.1 V/μs. This ramp is reset by a positive trigger pulse input which needs to be above 1 V amplitude and about 10 μs duration. The repetition rate of the trigger pulse input determines the amplitude of the ramp output, and at repetition rates below 5 kHz the ramp has time to reach the maximum possible positive level, which is a few volts below the +15 V supply. Note that the top of R_1 is then at a level well above the positive supply voltage.

Good linearity in the ramp output depends upon several factors in this circuit. The most important factor is that C_2 must be very large compared to C_1, because a change in voltage across C_2, during the ramp build up, will mean a departure from constant current in R_1. Other factors are leakage in Q_1 and leakage in C_1, which must be a high quality plastic film capacitor. All these factors tend to *reduce* the rate of rise of the ramp as its amplitude builds.

An interesting development of the bootstrap circuit can be tried out on the circuit shown in Fig. 7.12, which corrects for the factors listed above, and can, in fact, overcorrect for them and make the ramp *increase* its slope as its amplitude builds up. This development is to make the voltage follower, the CA3140, have a gain just above unity. This is easily arranged in Fig. 7.12 by adding another resistor, R_6, from pin 2 of the CA3140 down to ground. The resistor R_2 is only in Fig. 7.12, at the moment, to limit the current fed back to the inverting input: this is a recommendation on the CA3140 data sheet. When R_6 is added, R_2 plays a second role, and the voltage follower gain is increased from unity to $(1+R_2/R_6)$. Making $R_6 = 39\ \text{k}\Omega$, for example, will give a gain of 1.1, and a slight curving *upward* of the ramp output should be observed.

The trigger pulse input part of the experimental circuit, R_4 and R_5 in Fig. 7.12, has been made particularly simple because there are some very interesting observations to be made concerning the way in which the ramp actually begins.

When the positive trigger pulse arrives, Q_1 turns on and discharges C_1. The current is limited by R_3, assuming that Q_1 saturates rapidly, and the 'flyback' of the ramp should take place in well under 1 μs when the trigger pulse amplitude is above 1 V.

It is the duration of the positive trigger pulse which is the most interesting experimental variable. When the trigger pulse ends, Q_1 should turn off rapidly. The ramp should then begin, from a small positive level, the $V_{CE(SAT)}$ of Q_1, without any discontinuity in level, only a discontinuity in slope. A discontinuity in level will be seen, however, if the trigger pulse is not long enough to allow Q_1 to recover from the rather large current it passed during flyback and settle down to being saturated and passing only the rather small current flowing in R_1. This behaviour should be observed closely, because there is much to understand here.

7.14 Sine wave to square wave conversion

The final waveform generation problem to be considered in this chapter is a very classical one: the conversion of a sine wave into a fast square wave over a wide range of frequency, and with good correspondence between the zero crossings of the sine wave and the fast edges of the square wave.

A possible solution to this problem would be to build a wide-band amplifier and make it have a well-defined limiting action at its output stage. For example, suppose the input sine wave has an amplitude of 100 mV and the output is to be a square wave of 1 V amplitude. Further suppose that the rise and fall of the square wave must take up only 1 % of the total period. It follows that an amplifier with a gain of $1000/\pi$, just over 300, will be needed. This is a gain of 50 db and, glancing back at the data given in Fig. 6.1, it is clear that a gain of 50 db over a bandwidth of more than 10 MHz is not something which is easy to arrange. When this is coupled with the need for a well-defined limiting action in the output stage of this amplifier, which will produce negligible time delay in either going into its limit or coming out of it, the circuit design problems concerned with the sine wave to square wave conversion hardware begin to look quite formidable.

It is interesting, for the above reasons, to look at what can be achieved in this area by using one of the fast comparators which are available as

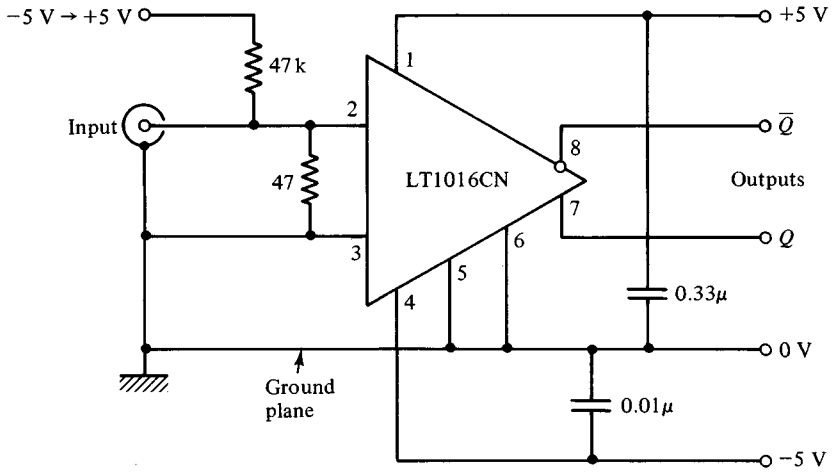

Fig. 7.13. *An experimental sine to square wave conversion circuit using a very fast comparator.*

integrated circuits. Comparator circuits were the subject of chapter 4 of this book, where the problem was one of capturing a very small input signal to the circuit at a well-defined time. Here the problem is one of amplification and limiting, but this is precisely what the simplest comparator circuits are designed to do. What is surprising about these devices is their remarkable bandwidth.

7.15 Experiments with a fast comparator

An example test circuit is shown in Fig. 7.13. This uses a fairly recent fast comparator: the LT1016 [20]. The experimental circuit shown in Fig. 7.13 is almost trivial in its simplicity, but it must be built very carefully with the LT1016 mounted over a ground plane, the two decoupling capacitors mounted with the shortest possible leads, and with the 47 Ω terminating resistor mounted as close to the device as possible. The output should be viewed with a wide bandwidth oscilloscope, using a passive 100:1 probe that loads the output with 5 kΩ.

The first test that should be made is an attempt to measure the small signal gain of the LT1016 and its small signal bandwidth. Connect an RF sinusoidal signal generator to the input and apply about 100 μV rms at 1 MHz. If the circuit has been constructed properly, it should then be possible to apply a voltage to the top of the 47 kΩ in Fig. 7.13 and bring the output level at either the Q or $\bar{Q}$ output, to a stable 1 V mean level. This is close to the output level at which the LT1016 should exhibit maximum small signal gain, and this gain should be about 70 db.

What is, perhaps, very unexpected about the LT1016, and, of course, other comparators of the same high quality, is the bandwidth over which this gain of 70 db is maintained. Increasing the input frequency will show an almost flat frequency response right out to around 20 MHz, where there may well be an increase in gain of several decibels before the gain collapses dramatically. Looking back at Fig. 6.1 shows that this performance is quite remarkable compared to the wide bandwidth operational amplifiers being discussed in chapter 6. In fact, 70 db is a gain of nearly 3500 so that its persistence up to 20 MHz could be interpreted as a gain-bandwidth product of 70 GHz. How is this possible with an integrated circuit fabricated using a bipolar process which gives transistors having cut-off frequencies of only a few gigahertz? The answer lies in the way in which the gain of the LT1016 rapidly collapses above 20 MHz. There is no gain at all at frequencies much above 20 MHz, and the LT1016 cannot be used with negative feedback to provide a well-defined wide-band gain.

The LT1016 has an output level limited between a few hundred millivolts above ground and about 4 V above ground. This makes the device compatible with standard logic and the limiting action is achieved with very little time delay. There is an excellent application note on the LT1016, which has been referred to before in this chapter [8].

The output limiting, and the function of the LT1016 as a solution to the sine wave to square wave conversion problem, may be studied by simply increasing the level of the sine wave input above the 100 μV which was used to check the small signal gain. Using an input sine wave of 100 mV peak, the LT1016 produces a good square wave at 10 MHz with the rise and fall times limited by the LT1016 to about 5 ns and the zero crossing of the square wave about 10 ns behind the zero crossing of the sine wave input. This 10 ns delay is the propagation delay of the LT1016 itself.

Reducing the input frequency, keeping the amplitude of the sine wave input constant at 100 mV, shows up what might be called the gain limited performance, as opposed to the speed limited performance which has just been seen at 10 MHz. Once the frequency is low enough to allow the LT1016 to reproduce the zero crossing of the input signal by means of its true small signal gain, the rise and fall times of the output square wave become input frequency dependent. A calculation along the lines of the one given at the beginning of section 7.14 shows that the rise and fall times will take up far less than 1 % of the total period, because of the high small signal gain of the LT1016. The thing for the experimentalist to watch out for, however, is just how the circuit behaves as the input level goes through zero, because it is here that any instability will be noticed. Instability can

be due to poor layout, poor component quality, or poor constructional technique.

7.16 Conclusions

The first experimental circuit in this chapter, the triangle waveform generator, operated at only audio frequencies. Despite this, a number of speed limitations could be seen: the gain and slew rate demands upon the operational amplifier being used as an integrator, the speed required from the comparator used in level control, and the speed limitations that might arise in the switching part of the circuit which brings about a reversal in the current supplied to the virtual earth of the integrator.

Output level control was discussed briefly in the section following this first experimental circuit. This is a vital factor when a triangle waveform is to be supplied to one of the triangle to sine wave conversion circuits, discussed in section 7.7, because the triangle wave amplitude must be kept constant over a very wide frequency range.

When precision waveform generation is called for, coupled with a need for high speed as well, the circuit design problems can get really difficult. Precision current sources, of the kind shown in Fig. 7.11, will solve precision waveform problems at low frequencies. Bootstrap techniques are more likely to give a solution at high speed, and a good illustration of this is the precision dual-slope DAC described by Mack, Horowitz and Blauschild [21]. In the experimental bootstrap circuit discussed in this chapter, Fig. 7.12, fine tuning of the ramp linearity could be illustrated by reducing the feedback across the voltage follower used there.

The chapter ended with an experiment that was rather unusual in comparison to the other experimental circuits in this book: the circuit detail was glossed over by treating the LT1016 fast comparator as a 'black box'. The circuit detail of the LT1016 is given, perhaps in a somewhat idealised form, in the data sheet [20], and it is well worth while spending some time understanding it.

Notes

1 Chiang, H. H., *Waveforming and Processing Circuits*, John Wiley, New York, 1986.
2 Neumann, U., Vogt, M., Brilhaus, F., and Husfeld, F., *Hewlett–Packard J.*, **38**, No. 4, 4–12, April 1987.
3 Gordon, B. M., *IEEE Trans. Circ. Syst.*, **CAS-25**, 396 and 405, 1978.
4 Rush, K., and Oldfield, D. J., *Hewlett–Packard J.*, **37**, No. 4, 7–8, April 1986.
5 Two excellent books almost cover this field: *Frequency Synthesizers: Theory and Design*, by V. Manassewitsch, John Wiley, New York, third edition, 1987, and *Frequency Synthesis by Phase Lock*, by W. F. Egan, John Wiley, New York, 1981.

6 Danielson, D. D., and Froseth, S. E., *Hewlett–Packard J.*, **30**, No. 1, 18–26, Jan 1979.
7 O'Dell, T. H., *Electronic Circuit Design: Art and Practice*, Cambridge University Press, Cambridge, 1988, pp. 107–10.
8 Williams, J. M., High Speed Comparator Techniques, in: *Linear Applications Handbook*, Linear Technology Corp., Milpitas, California, 1986, pp. 13.1–13.32.
9 These would be multilayer ceramic capacitors, between 0.1 μF and 0.47 μF, of the lowest possible voltage rating in order to get the smallest possible size. The dielectric would be X7R or Z5U.
10 Examples of such devices are the 5 V REF50Z, and 2.5 V REF25Z, made by Plessey; the 6.9 V LM329, made by National Semiconductor; and a number of so-called band-gap references which all give a reference voltage close to 1.2 V. All these devices work over a much wider current range, and have a temperature coefficient several orders of magnitude better, than simple Zener diodes.
11 O'Dell, T. H., *Electronic Engineering*, **61**, No. 753, 28 September 1989.
12 Ritchie, C. C., and Young, R. W., *Electronic Engineering*, **31**, 347–51, June 1959.
13 For example, the Hewlett–Packard 3312A Function Generator uses a 12 diode shaper circuit, which gives less than 0.5% distortion below 50 kHz. Details of this shaper are given by R. J. Riedel and D. D. Danielson, *Hewlett–Packard J.*, **26**, No. 7, 18–24, March 1975.
14 Gilbert, B., *IEEE J. Sol. St. Circ.*, **SC-17**, 1179–91, 1982.
15 Gilbert, B., *Electronics Letters*, **13**, 506–8, 1977.
16 Gilbert, B., *Electronics Letters*, **11**, 14–16 and 136, 1975.
17 The AD639 Universal Trigonometric Function Generator from Analog Devices is an example. This can provide an output proportional to $[\sin(x_1-x_2)]/[\sin(y_1-y_2)]$, where x_1, x_2, y_1 and y_2 are all signal inputs. In the simple triangle to sine wave conversion application, the AD639 can work quite accurately over an input range corresponding to $\pm 5\pi/2$, and may, therefore, be used as a frequency doubler or tripler into the bargain. The device is described on pages 3.123–3.134 of the *1986 Update and Selection Guide*, published by Analog Devices, Norwood, Massachusetts.
18 Buchanan, J. E., *IEEE Trans. Instr. Meas.*, **IM-24**, 33–9, 1975.
19 Ridenour, L. N. (Ed.), *Waveforms*, McGraw Hill, New York, 1949, pp. 267–78.
20 *1986 Linear Databook*, Linear Technology Corp., Milpitas, California, p. 5.36.
21 Mack, W. D., Horowitz, M., and Blauschild, R. A., *IEEE J. Sol. St. Cir.*, **SC-17**, 1118–26, 1982.